DOI: 10.13009/EUCASS2017-69

DOI: 069

Implications of Cycle Variants, Propellant Combinations and Operating Regimes on Fatigue Life Expectancies of Liquid Rocket Engines

Günther Waxenegger⋆*, Jörg Riccius*⋆*, Evgeny Zametaev*⋆*, Jan Deeken*⋆ *and Julia Sand*⋆
⋆*German Aerospace Center (DLR), Germany*
Im Langen Grund, 74239 Hardthausen am Kocher, Germany
guenther.waxenegger@dlr.de

Abstract

The paper in hand thematises a fatigue life analysis methodology for liquid rocket engines, with maiden focus on the combustion chamber. The method of analysis combines the engine cycle modelling tool Ecosim-Pro/ESPSS with 2-d Finite Element analysis methods developed by DLR's Institute of Space Propulsion. From the starting point of a generic LOx/LH_2 engine three objectives are pursued, changing the power cycle, the propellant combination to LOx/LCH_4 and lowering the chamber pressure. The results of the trade-off study focusing on the fatigue life expectancy are presented in detail.

1. Introduction

The (partial) reusability of launch systems provides a possibility of significantly reducing the costs associated with rocket launches. Currently technically feasible concepts of reusability focus on reusable booster stages. With the Falcon 9 launch vehicles, SpaceX demonstrated its ability to successfully return the first stages of orbital launchers. Furthermore, SpaceX conducted a re-flight of a recovered first stage in March 2017 and once again landed the booster. In order to bring down the costs, it is absolutely necessary to reduce the required refurbishment to a minimum. This is particularly true of the engines which are responsible for a large fraction of the total stage cost.[4] To make things worse the propulsion system belongs to the most critical subsystems of a launch system.[7] This is driven by the extreme operational load conditions to which the system is exposed during operation. It follows that cost-effective reusability of booster engines is a key technology for (partial) reusability of launch systems.

Therefore, a detailed understanding of the failure mechanisms and the influence of essential design choices like the cycle variant as well as the propellant combination on the fatigue life expectancy of liquid rocket engines is desirable. Design parameters like the chamber pressure also have significant implications for the fatigue life.

Copyright © 2017 by Waxenegger, Riccius, Zametaev, Deeken and Sand. Published by the EUCASS association with permission.

DOI: 10.13009/EUCASS2017-69

1.1 Methodology

This section describes the methods used for the following investigation. The baseline for each life expectancy calculation is a careful analysis of the engine cycle. Engine cycle analysis is invaluable, enables a rough estimation of the engine's specific impulse and allows the definition of the interfaces between the engine and the launch vehicle in terms of high level parameters. In addition the chosen cycle has a decisive influence on the fatigue life. To show this, 2-d finite element analysis methods are utilized, which use the previously generated cycle analysis results as input values. The fatigue life expectancy of the engine can be estimated by determining the fatigue life expectancy of the individual components. Components exposed to high loads are for example the turbomachinery and the combustion chambers.[11] Calculation methods which focus on the expected fatigue life of the main combustion chamber are already several years in development at DLR's Institute of Space Propulsion and have been continuously improved.[9]
Recall that the combustion chamber of a cryogenic rocket engine is exposed to serious thermal and mechanical loads during operation.[8] The thermal loads consist basically of two contributions. First, there is a large temperature difference between the hot gas side and the coolant side of the chamber wall, which tries to bend the internal shell. Second, there is an even larger temperature difference between the inner liner and the stiff external outer jacket. The resulting thermal stresses are usually beyond the elastic limit of the copper alloy used for the inner liner. The mechanical loads are due to the pressure differences between the interior of the chamber and the cooling channels at a certain axial position. The pressure in the cooling channels is among other things dependent on the required exit pressure at the outlet of the regenerative cooling and thus also the cycle choice plays a decisive role.

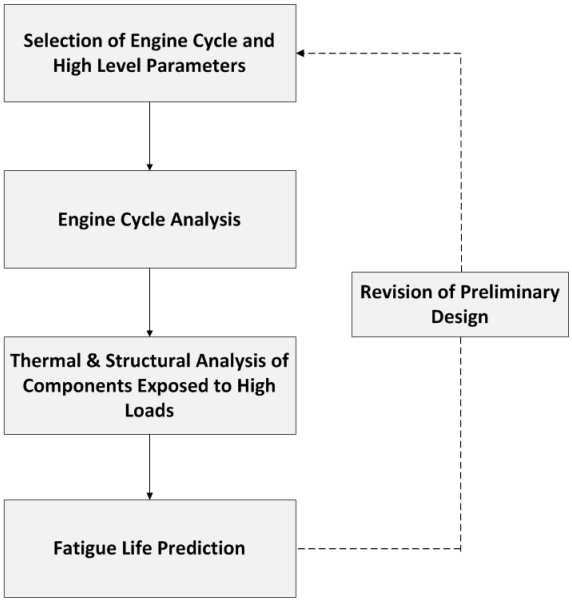

Figure 1: Process Cycle

1.2 Cycle Analysis with EcosimPro/ESPSS

The cycle analysis is carried out with the simulation tool EcosimPro, developed by EA Internacional. It is designed to model complex physical processes and 0-d and 1-d mathematical models. Both continuous and discrete systems can be modelled. The software contains an object-orientated programming language and a user-friendly graphical user interface. The graphical user interface enables to combine different components, which are arranged in several libraries. Of particular interest are the European Space Propulsion System Simulation (ESPSS) libraries, which are commissioned by the European Space Agency (ESA). These EcosimPro libraries are suited for the simulation of liquid rocket engines and have been constantly upgraded in recent years. In order to improve the quality of the results, it is nevertheless indispensable to add more detailed calculation methods for certain components. Fortunately, this can be easily done thanks to the open software architecture. For example, the original heat transfer calculation present in the ESPSS library is modified in such a way that the expected efficiency of the cooling ribs is better reproduced. EcosimPro/ESPSS allows to analyse steady and transient conditions, e.g. start-up and shutdown of an engine. For the preliminary trade-off study steady state simulations are sufficient.

DOI: 10.13009/EUCASS2017-69

1.3 Thermal & Structural Analysis with ANSYS

The basis for the 2-d Finite Element analysis is formed by the values of certain key parameters, in part generated by the cycle analysis, as for example the pressure in the chamber and the cooling channels, the temperature on the hot and cold gas side, as well as the cooling channel geometry at the nozzle throat cross section. The failure of the chamber wall is assumed to occur in this cross section.The following analysis focuses on a half cooling channel + half rib model of a chamber wall section at the nozzle throat. The combustion chamber wall is assumed to have a Copper alloy inner liner and a galvanically deposited Nickel outer shell. Figure 2 (a) shows the boundary conditions used for the thermal analysis. As approximation a linear temperature decrease to the temperature of the coolant is assumed.

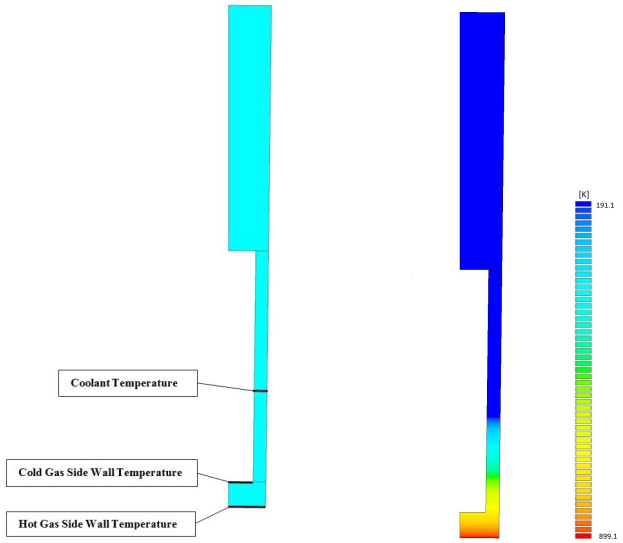

(a) Boundary Conditions

(b) Temperature Profile during Operation

Figure 2: Thermal Analysis

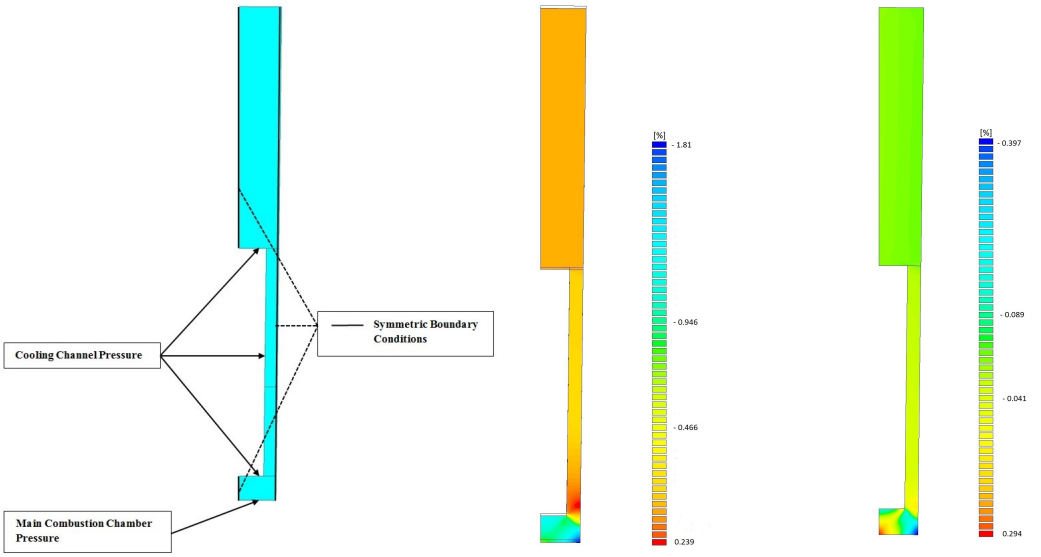

(a) Boundary Conditions

(b) Strain Profile during Operation

(c) Strain Profile after Operation

Figure 3: Structural Analysis

DOI: 10.13009/EUCASS2017-69

The boundary conditions for the structural analysis are given by the loads due to the pressures which are present in the main combustion chamber and cooling channels as well as symmetry conditions. Elasto-plasticity according to the rate independent version of the Chaboche model with kinematic hardening and isotropic softening for T = 900 K and additionally isotropic hardening for the first few cycles for the temperature levels of T = 300 K, T = 500 K and T = 700 K is selected for the structural Finite Element analysis of the chamber wall cut-out.[10] For efficiency reasons, just the very first loading cycle of the engine (first pre cooling, first hot run, first post cooling and relaxation back to ambient condition) is modelled by the Finite Element method.

1.4 Fatigue Life Prediction

For the assumed failure node of the Finite Element model, the minimum strain ϵ_{min}, the maximum strain ϵ_{max} and the strain ϵ_{end} at the end of the loading cycle is extracted from the 2-d Finite Element analysis solution field and taken into account by the following post processing procedure:
The cyclic strain difference $\triangle\epsilon = \epsilon_{max} - \epsilon_{min}$ is used as the main input value for the temperature dependent Coffin-Manson model, resulting in the number of cycles-to-failure $N_{LCF,CoffMans}(\triangle\epsilon, T)$ in the absence of any ratcheting deformation. The Coffin-Manson usage factor $u_{CoffMans}(\triangle\epsilon, T)$ is then defined as the reciprocal value of the number of cycles-to-failure determined by the Coffin-Manson method:

$$u_{CoffMans}(\triangle\epsilon, T) = \frac{1}{N_{LCF,CoffMans}(\triangle\epsilon, T)}. \tag{1}$$

The temperature dependent ratcheting caused ductile failure usage factor $u_{ratch}(\epsilon_{end}, \epsilon_{ult}(T))$ is defined by:

$$u_{ratch}(\epsilon_{end}, \epsilon_{ult}(T)) = \frac{max(0, \epsilon_{end})}{\epsilon_{ult}(T)}, \tag{2}$$

with $\epsilon_{ult}(T)$: The temperature dependent ultimate strain of the chamber wall material. Then, the two usage factors are summed up to get the (temperature dependent) total usage factor $u_{total}(T)$:

$$u_{total}(T) = \frac{1}{N_{LCF,CoffMans}(\triangle\epsilon, T)} + \frac{max(0, \epsilon_{end})}{\epsilon_{ult}(T)}. \tag{3}$$

Finally, the total number of cycles-to-failure $N_{LCF,total}$ (combining Low Cycle Fatigue according to Coffin-Manson with the ratcheting caused ductile failure of the structure) is determined as the reciprocal value of the total usage factor:

$$N_{LCF,total}(T) = \frac{1}{\frac{1}{N_{LCF,CoffMans}(\triangle\epsilon,T)} + \frac{max(0,\epsilon_{end})}{\epsilon_{ult}(T)}}. \tag{4}$$

The implemented method allows to examine the direct impact of design decisions on the fatigue life expectancy of the main combustion chamber. It would be desirable to have analogous methods for determining the fatigue life expectancy of the turbomachinery (especially the turbines) at one's disposal. For the turbines the load cases include among other things rotational loads, thermal loads as well as mechanical loads due to the pressure differences along the blades.[11] The difficulty is that the estimation should only include the implications which are present in the generic case and not focus on some detailed design. Such a correlation is at the moment out of scope. Nevertheless simple implications are obvious, e.g. in terms of the life expectancy higher turbine inlet temperatures are not favourable.

DOI: 10.13009/EUCASS2017-69

2. Investigated Cycle Variants

This section describes the considered engine cycle variants. The focus of this study are liquid rocket engines suitable for the first stage application of orbital launchers. Therefore, the chosen cycles for the analysis of fatigue life expectancies are on the one hand two open cycles; the gas generator and the expander bleed,[2] and on the other hand two closed cycles; the fuel rich staged combustion and the full flow staged combustion.[5] All of the above mentioned engine cycles have a realistic potential to be chosen for a new engine development or are already state of the art for launcher propulsion systems. In addition to the comparison of the cycles, the analysis has been carried out with two cryogenic propellant combinations, LOx/LH_2 and LOx/LCH_4. LOx/LH_2 is the currently favoured propellant combination in Europe and is used in a wide range of rocket engines. However, methane as fuel is under investigation at many space agencies and in the industry all over the world and could have significant benefits compared to hydrogen.[6]

The baseline for this study is a LOx/LH_2 engine with a chamber pressure of 100 bar, generating a vacuum thrust of 1000 kN and employing a gas generator cycle. This generic engine is not linked to any existing development project. From this starting point three objectives are pursued, changing the power cycle, the propellant combination and lowering the chamber pressure. All engines are designed to achieve a vacuum thrust of 1 MN and the nozzle expands to a ambient pressure of $p_e = 0.4$ bar.

The most important parameters of each cycle are displayed in the tables below.

Table 1: Main Parameters

Parameter	**LOx/LH_2**	**LOx/LCH_4**
Combustion Chamber Mixture Ratio [-]	6	3.4
Main Combustion Chamber Pressure [bar]	100	100
Vacuum Thrust Level [kN]	1000	1000
Turbomachinery Efficiency [-]	0.7	0.7

Table 2: Open Cycle - Parameters

Parameter	**Gas Generator**		**Expander Bleed**
	LOx/LH_2	LOx/LCH_4	
Gas Generator Mixture Ratio [-]	0.97	0.375	-
Turbine Pressure Ratio [-]	20	20	20
Turbine Inlet Temperature [K]	991.82	994.10	251.89

Table 3: Closed Cycles - Parameters

Parameter	**Fuel Rich Staged Combustion**	**Full Flow Staged Combustion**
LOx/LH_2		
Oxidizer Rich Preburner Mixture Ratio [-]	-	171
Fuel Rich Preburner Mixure Ratio [-]	0.645	0.495
Turbine Pressure Ratio [-]	1.217	1.217
LOx-Turbine Inlet Temperature [K]	770.49	592.38
LH_2-Turbine Inlet Temperature [K]	770.49	625.05

DOI: 10.13009/EUCASS2017-69

FATIGUE LIFE EXPECTANCIES

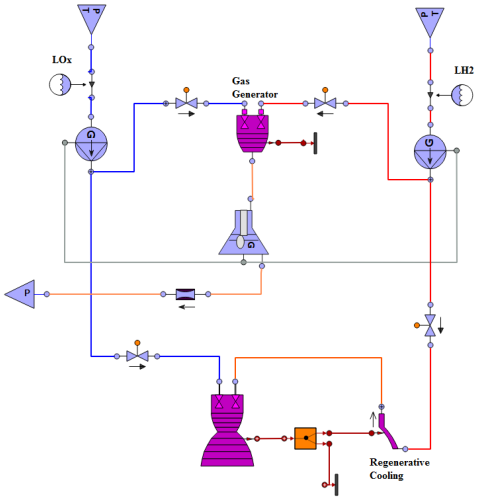

(a) Schematic of Gas Generator Cycle

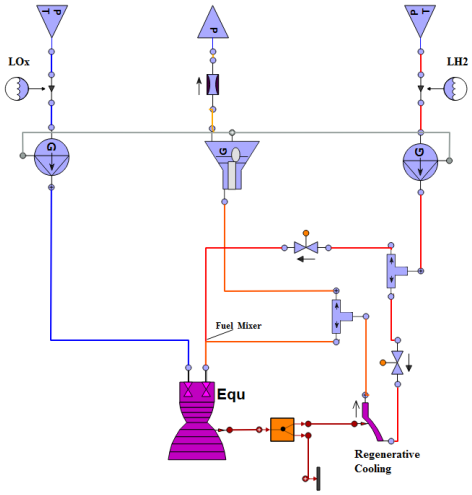

(b) Schematic of Expander Bleed Cycle

Figure 4: Schematics of Open Cycles

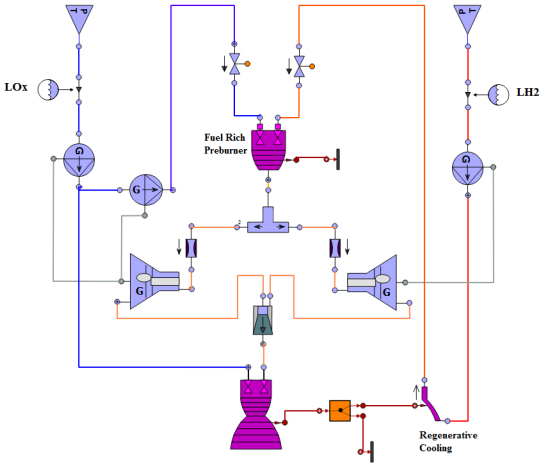

(a) Schematic of Fuel Rich Staged Combustion Cycle

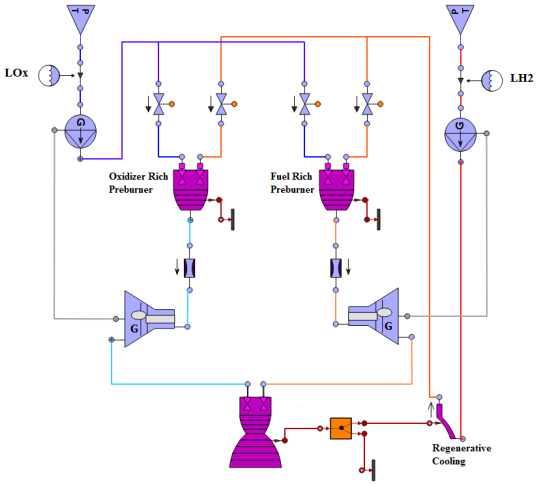

(b) Schematic of Full Flow Staged Combustion

Figure 5: Schematics of Closed Cycles

DOI: 10.13009/EUCASS2017-69

3. Design Logic

3.1 Design Logic of Combustion Chamber and Nozzle

The design logic of the combustion chambers and the nozzles of the different cycles is based on the targeted performance characteristics of the rocket engines, which are the thrust level, the pressure and the mixture ratio in the main combustion chamber. Besides, additional parameters are fixed to enable the comparison of the engines; the contraction ratio, the characteristic length, the design contour of the main combustion chamber and the nozzle and the ambient pressure.

With the help of NASA's Chemical Equilibrium with Applications (CEA) and the fixed performance values the thrust coefficient c_F, the characteristic velocity c^* and the area expansion ratio ε are calculated. As a consequence, by using the following equations the throat section of the engines is calculated, which is the baseline for the chamber and nozzle design:

$$F = \dot{m}\, I_{sp} = \dot{m}\, c_F\, c^*, \tag{5}$$

$$c^* = \frac{A^*\, p_C}{\dot{m}}, \tag{6}$$

where $\dot{m}$ denotes the chamber mass flow rate, I_{sp} the specific impulse, A* the critical section area and p_c the pressure in the main combustion chamber.
The design of the contour of the main combustion chamber and the nozzle is based on the values published by Huzel[3] and created with CAD. The combustion chamber is assumed to be a cylindrical chamber including a bottleneck section until the throat. Additionally, the characteristic length of the main combustion chamber for all cycles is determined to $L^*_{H_2} = 700$ mm for hydrogen and $L^*_{CH_4} = 800$ mm for methane. The volume of the cylindrical and the bottleneck part are dimensioned to fit the defined characteristic length. An expander bleed cycle does not have a gas generator and preburner respectively; the turbomachinery is driven by a fraction of the propellant that picked up heat energy in the cooling channels of the regenerative cooling. To increase this heating the length of the chamber is typically increased compared to the chamber length of a gas generater cycle with the same chamber pressure. In order to guarantee a realistic expander bleed simulation, the chamber length of the expander bleed cycle was set to be four times the diameter of the chamber.

The nozzles are based on a parabolic approximation of a bell nozzle based on a 15° conical nozzle and are designed according to Figure 6.

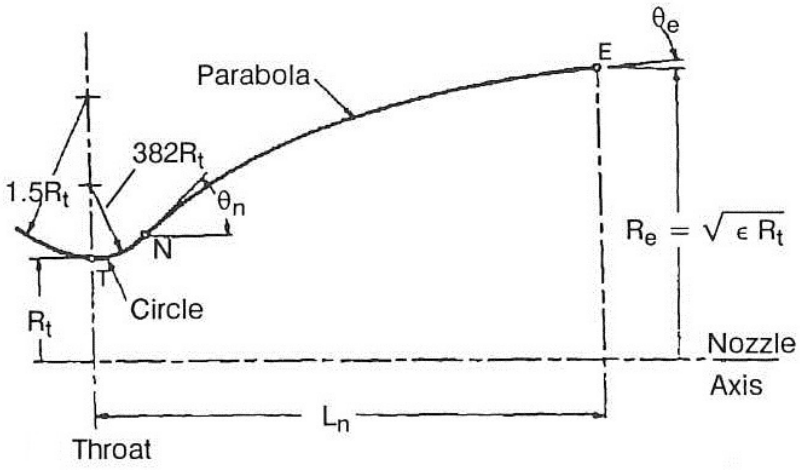

Figure 6: Parabolic Approximation of Bell Nozzle Contour

DOI: 10.13009/EUCASS2017-69

The most important geometric parameters are displayed in Table 4.

Table 4: Geometric Parameters

Parameter	**Gas Generator**		**Expander Bleed**	**Closed Cycles**
	LOx/LH_2	LOx/LCH_4		
Throat Diameter [mm]	264.1	263.2	264.1	264.1
Contraction Ratio [-]	2.3	2.3	2.3	2.3
Expansion Ratio [-]	25.04	27.89	25.04	25.04
Chamber Length [mm]	376	418	1602.1	376

3.2 Design Logic of Regenerative Cooling

Assuming a fixed propellant combination and chamber pressure, the cooling channel geometry is the same for the considered gas generator, fuel rich staged combustion and full flow staged combustion cycles and the exact dimensions can be extracted from Table 5. Only the geometry of the expander bleed cycle cooling channels differs from these values, due to the fact that the coolant mass flow rate is reduced to increase the specific heat up and thereby the efficiency of the engine. Table 6 shows the cooling channel geometry for the LOx/LH_2 expander bleed cycle. The different height of the cooling channels guarantees that the the maximum temperature of the combustion chamber wall equals 900 K at the nozzle throat for each case. Furthermore, the regenerative cooling always starts at an area expansion ratio of $\varepsilon = 15$ and streams in counter-flow direction until the chamber inlet.

Table 5: Cooling Channel Geometry - LOx/LH_2

Parameter	**Unit**	**Value**
Number of Cooling Channels	-	276
Cooling Channel Width	mm	2
Cooling Channel Height	mm	23.8
Inner Wall Thickness	mm	1

Table 6: Cooling Channel Geometry - LOx/LH_2 - Expander Bleed

Parameter	**Unit**	**Value**
Number of Cooling Channels	-	276
Cooling Channel Width	mm	2
Cooling Channel Height	mm	20.35
Inner Wall Thickness	mm	1

DOI: 10.13009/EUCASS2017-69

4. Results

Within this section the achieved results of the study are discussed and the values of importance are displayed in the tables below.

Table 7: Performance Levels

Engine Cycles	**I_{sp} [s]**	**Expected Numbers of Cycles [-]**	**Turbine Inlet Temperature [K]**	
			Turbine 1	Turbine 2
LOx/LH_2				
Gas Generator	418.68	66	991.82	-
Expander Bleed	403.36	54	251.89	-
Fuel Rich Staged Combustion	425.03	49	770.49	770.49
Full Flow Staged Combustion	425.02	50	592.38	625.05
LOx/LCH_4				
Gas Generator	330.75	71	994.13	-

Table 8: Cooling Channel Pressures

Engine Cycle	**Cooling Channel Pressure [bar]**
LOx/LH_2	
Gas Generator	121.32
Expander Bleed	154,33
Fuel Rich Staged Combustion	166.83
Full Flow Staged Combustion	165.37
LOx/LCH_4	
Gas Generator	138.34

The results in Table 7 show, that for our assumptions the combustion chamber of the gas generator cycle has the highest number of cycles-to-failure, more precisely an expected number of 66 cycles. It is followed by the expander bleed cycle with 54 expected cycles-to-failure. The staged combustion cycles possess an even lower number of expected cycles-to-failure, namely 49 cycles and 50 cycles respectively. The cause for this result is the different pressure present in the cooling channels at the throat. In case of the expander bleed cycle the higher cooling channel pressure is necessary due to the increased chamber length and the decreased coolant mass flow rate. The pressure in the cooling channels is also higher for the staged combustion cycles. In this case, the reason is the higher exit pressure required at the outlet, because the fuel enters the high pressure preburners after leaving the cooling. Thus the mechanical loads are increased compared to the gas generator cycle.

It is important to emphasize that the mechanical loads due to the pressure differences are usually secondary and that the primary influence on the fatigue life of the combustion chamber is given by the thermal loads. Due to the boundary condition of 900 K as the maximum chamber wall temperature, the thermal loads at the throat of the combustion chamber are almost similar for each cycle variant, see Table 9. This circumstance is easy to understand. The thermal loads depend on the heat flux, the material selection and the cooling channel geometry. In this trade-off study the material selection is assumed to be fixed. The cooling channel height is slightly reduced for the expander bleed cycle to achieve the same cooling efficiency for a reduced cooling mass flow rate. Apart from that, the cooling channel geometry is also assumed to be fixed. A small difference is caused by the slightly different coolant temperatures which lead to a heat flux change.

Clearly, the cycle selection has a great influence on the turbomachinery. Table 7 shows that the turbine inlet temperature of the expander bleed cycle is quite low, which should lead to a high life expectancy of the turbine, but greatly reduces the performance of the engine. To increase the specific heat pick up of the coolant further and thereby improve

DOI: 10.13009/EUCASS2017-69

Table 9: Temperature Levels

Engine Cycle	**Wall Temperature [K]**		**Coolant Temperature [K]**
	Hot Gas Side	Cold Gas Side	
LOx/LH_2			
Gas Generator	899.80	732.59	83.05
Expander Bleed	899.32	733.06	96.09
Fuel Rich Staged Combustion	896.24	729.32	89.76
Full Flow Staged Combustion	896.22	729.31	89.55
LOx/LCH_4			
Gas Generator	899.31	749.17	194.10

the performance one could use a split cooling. As distinguished from the full counter-flow cooling the cooling jacket is then divided into an upper and lower part for the second cooling variant. The coolant inlet is downstream of the throat in both cases but for the second variant the inlet is near the throat. After cooling the entire subsonic part of the thrust chamber in counter-flow direction the coolant or rather a portion of it is used to cool the upper divergent part of the nozzle (in co-flow direction), where the cooling does not need to be as efficient. In this way one can significantly increase the temperature of the coolant at the inlet of the turbine.[1] The same trade-off between life expectancy and performance applies to the gas generator cycle. By increasing the gas generator temperature one improves the performance of the cycle, but the thermal loads on the turbine grow as well and thus the expected fatigue life is reduced. The staged combustion cycles feature the highest specific impulses and for the assumed chamber pressure the required turbine inlet temperatures are quite moderate. Because all the fuel and all the oxidizer are going through the turbine(s), the turbine(s) can run at an even lower temperature in the full flow staged combustion cycle.

It is frequently claimed that the propellant combination LOx/LCH_4 is better than LOx/LH_2 in terms of the expected fatigue life of the combustion chamber.[6] Our results confirm this statement. Table 7 shows that for our assumptions switching the propellant combination from LOx/LH_2 to LOx/LCH_4 causes an increase of the number of cycles-to-failure from 66 to 71. The main reason for this is given by the different temperatures of the propellants when used as coolant. In contrast to hydrogen, which in our cycle analysis has a temperature of 83 K inside the cooling channels at the nozzle throat section, methane has a temperature of 194 K. This circumstance leads to significantly reduced thermal loads. But one has to accept a higher pressure drop compared to hydrogen to maintain the same maximum wall temperature when using methane in the regenerative cooling. Thus the mechanical loads due to the pressure differences are increased. Nevertheless the positive effect of the reduced thermal loads outweighs the impact of the higher pressure inside the cooling channels concerning the life expectancy of the combustion chamber.

It is well known that the use of LOx/LH_2 offers the highest specific impulse. This is also reflected in the results in table 7, where we adjusted the mixture ratio of the gas generator to get around 1000 K at the inlet of the turbine in both cases.

Please note that the results do not imply that for fixed thrust and chamber pressure the propellant combination LOx/LCH_4 always leads to an increased number of cycles-to-failure. This is only true, when one chooses the same maximum wall temperature at the hot gas side. However one could reduce the maximum temperature at the hot gas side of the combustion chamber wall by modifying the regenerative cooling, e.g. by changing the height of the cooling channels, to get an extended life expectancy. A reduced maximum wall temperature typically implies a higher pressure drop in the cooling channels which results in a lower performance of the engine. In other words, the results show that requiring a certain minimum number of expected cycles-to failure can force a necessary reduction of the performance of a liquid rocket engine and that this reduction depends on the propellant choice.

Finally, the implications of choosing a different nominal chamber pressure are taken into account, displayed in the Tables 10,11 and 12. For chamber pressures of 90 bar and 80 bar, the numbers of cycles-to-failure are 67 and 69 respectively. These results show, that in terms of life expectancy lower chamber pressures are favourable. Lowering the chamber pressure leads to reduced heat fluxes as well as lower mechanical loads due to smaller pressure differences between the interior of the chamber and the cooling channels.

DOI: 10.13009/EUCASS2017-69

Table 10: Performance Levels by Variable Pressures

Main Chamber Pressure [bar]	**I_{sp} [s]**	**Expected Numbers of Cycles [-]**	**Turbine Inlet Temperature [K]**
80	415.46	69	996.52
90	417.27	67	998.59
100	418.68	66	991.82

Table 11: Temperature Levels by Variable Pressures

Main Chamber Pressure [bar]	**Wall Temperature [K]**		**Coolant Temperature [K]**
	Hot Gas Side	Cold Gas Side	
80	900.07	781.37	75.24
90	899.14	756.20	79.29
100	900.20	743.59	77.19

Table 12: Cooling Channel Pressure by Variable Pressures

Main Chamber Pressure [bar]	**Cooling Channel Pressure [bar]**
80	93.45
90	107.05
100	119.42

5. Summary and Outlook

The comparison of different cycle variants at fixed chamber pressure and thrust level revealed interesting results. First, not taking into account a possible change of the maximum temperature of the main combustion chamber wall, the study showed that the gas generator cycle led to the highest expected number of cycle-to-failure for the combustion chamber. A possible reduction of the maximum wall temperature offers an inherent trade-off between the expected fatigue life on one side and the possible performance of the liquid rocket engine on the other side. Further studies are planned to systematically analyse this trade-off for different initial situations. Furthermore, the methods will allow the design of liquid rocket engines with a fixed fatigue life expectancy, e.g. 100 cycles for sensible reusable launch vehicle concepts. In addition to that future optimizations of engines should take the fatigue life expectancy of certain components into account.

As discussed in detail in the previous section the propellant combination LOx/LCH_4 yields certain advantages in relation to the fatigue life expectancy of a combustion chamber. Finally, the results also showed that the operating regime has a significant influence on the loads which act on the critical subcomponents. Choosing a medium performance version of a potential high performance architecture could be ideal with regard to reusable launch systems.

Main open points include advanced methods for the estimation of the fatigue life of cycle specific, but otherwise generic, turbomachinery. Regarding life expectancy enhancement of combustion chambers as well as turbomachinery, the implications of using additional film cooling should also be the focus of future studies.

6. Acknowledgments

It is a pleasure to thank A. Herbertz, D. Greuel and R. Dos Santos Hahn for many useful discussions.

DOI: 10.13009/EUCASS2017-69

References

[1] J. Deeken and G. Waxenegger. LUMEN: Engine Cycle Analysis of an Expander-Bleed Demonstrator Engine for Test Bench Operation. *DLRK*, 2016.

[2] A. Herbertz, J. Kauffmann, and M. Sippel. Systems Analysis of a Future Semi-Reusable Launcher, Based on a High Thrust Bleed Cycle Rocket Engine. *Joint Propulsion Conference*, 2001.

[3] D. K. Huzel and D. H. Huang. *Modern Engineering for Design of Liquid-Propellant Rocket Engines*. American Institue of Aeronautics and Astronautics, Inc., 1992.

[4] D. E. Koelle. *Handbook of Cost Engineering and Design of Space Transportation Systems*. TCS - TransCostSystems, 2013.

[5] D. Manski, C. Goertz, H.-D. Saßnick, J. R. Hulka, B. D. Goracke, and D. J. H. Levack. Cycles for Earth-to-Orbit Propulsion. *Journal of Propulsion and Power*, 14(5):588–604, September-October 1998.

[6] D. Preclik, G. Hagemann, O. Knab, L. Brummer, C. Mäding, D. Wiedmann, and P. Vuillermoz. LOX/Hydrocarbon Propellant Trade Considerations for Future Reusable Liquid Booster Engines. *Joint Propulsion Conference*, 2005.

[7] D. Preclik, R. Strunz, G. Hagemann, G. Hangel, and W. Zinner. Reusability Aspects for Space Transportation Rocket Engines: Programmatic Status and Outlook. *DLRK*, 2010.

[8] J. Riccius. Wärmeübergang, Kühlung, Lebensdauer - Optimierung von Raketenbrennkammern. *DGLR*, 2002.

[9] J. Riccius, W. Bouajila, and E. Zametaev. Comparison of Finite Element analysis and experimental results of a combustion chamber type TMF panel test. *Joint Propulsion Conference*, 2013.

[10] J. Riccius, E. Zametaev, W. Bouajila, and Q. Wargnier. Inner liner temperature variation caused deformation localization effects in a multichannel model of a generic LRE wall structure. *Propulsion and Energy*, 2014.

[11] M. Rudis and J. Riccius. Liquid Rocket Engine Component Failure Probability and Residual Life Prediction at Thermal and Mechanical Cyclic Loading. *ECCOMAS*, 2004.